

# Soft X-ray Absorption and X-ray Photoelectron Spectroscopic Study of Tautomerism in Intramolecular Hydrogen Bonds of *N*-Salicylideneaniline Derivatives

Eisuke Ito,<sup>\*,1a</sup> Hiroshi Oji,<sup>1a</sup> Tohru Araki,<sup>1a,b</sup> Kazuyoshi Oichi,<sup>1a</sup> Hisao Ishii,<sup>1c</sup> Yukio Ouchi,<sup>1a</sup> Toshiaki Ohta,<sup>1d</sup> Nobuhiro Kosugi,<sup>1c</sup> Yusei Maruyama,<sup>1e</sup> Toshio Naito,<sup>1f</sup> Tamotsu Inabe,<sup>1f</sup> and Kazuhiko Seki<sup>1a</sup>

Contribution from the Department of Chemistry, Graduate School of Science, Nagoya University, Furo-cho, Chikusa-ku, Nagoya 464-01, Japan, Photon Factory, National Laboratory for High Energy Physics, Oho, Tsukuba, Ibaraki 305, Japan, Institute for Molecular Science, Myodaiji, Okazaki 444, Japan, Department of Chemistry, Graduate School of Science, The University of Tokyo, Hongo, Bunkyo-ku, Tokyo 113, Japan, Department of Materials Chemistry, College of Engineering, Hosei University, Kajino-cho, Koganei, Tokyo 184, Japan, and Department of Chemistry, Graduate School of Science, Hokkaido University, Sapporo 060, Japan

Received December 2, 1996. Revised Manuscript Received March 25, 1997<sup>®</sup>

**Abstract:** The tautomerism in solid phase was studied by near-edge X-ray absorption fine structure (NEXAFS) spectroscopy at the N *K*- and O *K*-edges and X-ray photoelectron spectroscopy (XPS) in the N1s and O1s regions for five *N*-salicylideneaniline derivatives: *N,N'*-disalicylidene-1,6-pyrenediamine (DSPY), *N,N'*-disalicylidene-*p*-phenylenediamine (BSP), *N*-(2-hydroxy-1-naphthylidene)-1-pyrenylamine (NPY), *N,N'*-di(2-hydroxy-1-naphthylidene)-*p*-phenylenediamine (DNP), and the complex between DNP and 7,7,8,8-tetracyanoquinodimethane (DNP-TCNQ). The NEXAFS spectral features were assigned by (1) the comparison with the core excitation spectra of reference compounds and (2) ab initio MO calculations of the core-excited states by the improved virtual orbital method using the relaxed Hartree–Fock orbitals. The tautomeric structures were deduced by the intensity of peaks characteristic of the tautomers in OH- and NH-forms. The XPS spectra gave structures consistent with those by NEXAFS and also allowed quantitative estimation of the relative tautomer populations. The results range from the dominance of the OH-form in DSPY and BSP to a comparable mixture of the OH- and NH-forms in DNP and DNP-TCNQ. These structures are consistent with the previous estimation by X-ray diffraction (XD), except for DNP-TCNQ where XD suggested the NH-form dominance. The good correlation of the population by XPS with the C–O bond length by XD supports the present conclusion for DNP-TCNQ. These results demonstrate the usefulness of NEXAFS as well as XPS for studying the tautomerism in hydrogen bonded systems.

## 1. Introduction

*N*-Salicylideneaniline (SA) derivatives have long attracted attention due to their unique asymmetric intramolecular hydrogen (H-) bonds (O–H···N),<sup>2–4</sup> which often cause a double minimum potential well along the H atom coordinate.<sup>5</sup> As a result, some SA derivatives show tautomerism by proton transfer from oxygen (OH-form) to nitrogen (NH-form),<sup>2,6–8</sup> as shown in Figure 1.

Such proton transfer causes the change in the  $\pi$ -electron system. For using such compounds as electronically functional materials, Inabe and co-workers<sup>9–12</sup> studied the H-bonded

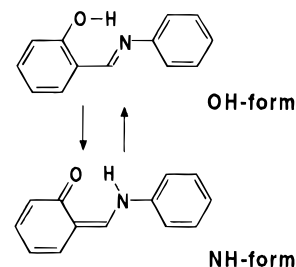


Figure 1. Tautomerism in *N*-salicylideneaniline.

structure of various SA derivatives by X-ray diffraction (XD) and infrared absorption (IR) spectroscopy. They concluded that (i) the tautomerism ranges from pure OH-form to almost pure NH-form<sup>9–11</sup> and (ii) H-bonded structure is sensitively affected by the intermolecular charge-transfer (CT) interaction.<sup>10–12</sup> These results showed that the electronic and the protonic states are actually strongly coupled.

However, ambiguity still remains even about the structure. The position of the proton has been estimated by XD using

(9) Inabe, T.; Luneau, I.; Mitani, T.; Maruyama, Y.; Takeda, S. *Bull. Chem. Soc. Jpn.* **1994**, *67*, 612–621.

(10) Inabe, T. *New J. Chem.* **1991**, *15*, 129–136.

(11) Inabe, T.; Okaniwa, K.; Okamoto, H.; Mitani, T.; Maruyama, Y. *Mol. Cryst. Liq. Cryst.* **1992**, *216*, 229–234.

(12) Inabe, T.; Hoshino-Miyajima, N.; Luneau, I.; Mitani, T.; Maruyama, Y. *Bull. Chem. Soc. Jpn.* **1994**, *67*, 622–632.

<sup>®</sup> Abstract published in *Advance ACS Abstracts*, June 1, 1997.

(1) (a) Nagoya University. (b) Photon Factory. (c) Institute for Molecular Science. (d) The University of Tokyo. (e) Hosei University. (f) Hokkaido University.

(2) Cohen, M. D.; Schmidt, G. M. J.; Flavian, S. *J. Chem. Soc.* **1964**, 2041–2051.

(3) Bregman, J.; Leiserowitz, L.; Schmidt, G. M. J. *J. Chem. Soc.* **1964**, 2068–2085.

(4) Bregman, J.; Leiserowitz, L.; Osaki, K. *J. Chem. Soc.* **1964**, 2086–2100.

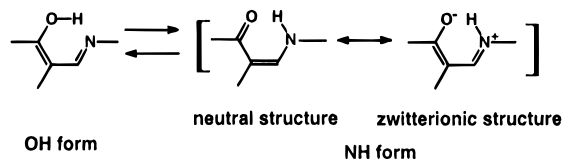
(5) Tayyari, S. F.; Zeegers-Huyskens, Th.; Wood, J. L. *Spectrochim. Acta* **1979**, *35A*, 1289–1295.

(6) Barbara, P. F.; Rentzepis, P. M.; Brus, L. E. *J. Am. Chem. Soc.* **1980**, *102*, 2786–2791.

(7) Higelin, D.; Sixl, H. *Chem. Phys.* **1983**, *77*, 391–400.

(8) Hoshino, N.; Inabe, T.; Mitani, T.; Maruyama, Y. *Bull. Chem. Soc. Jpn.* **1988**, *61*, 4207–4214.

## Scheme 1



D-synthesis,<sup>8–13</sup> but this method cannot give the definite position due to the small X-ray scattering factor. The IR results were not definite either,<sup>9,10,12</sup> since OH and NH stretching bands were blurred by the broadening due to H-bond formation. Thus studies by other reliable method have been desired.

Near edge X-ray absorption fine structure (NEXAFS) spectroscopy is a recently developed method, which examines inner shell electron excitations to various vacant states.<sup>14</sup> It offers information about chemical bonding around the excited atom. Also we can use the selection rules for 1s excitation<sup>14</sup> that the excitation is allowed only when (1) the final state has p-character and (2) the electric vector *E* of the light has a parallel component to the axis of the p orbital. These are useful for assigning the spectral features,<sup>14,15</sup> if one can use an oriented sample and polarized light. Using these characteristic aspects, we can study the H-bonded structure in SA derivatives by NEXAFS spectroscopy by examining the excitations to the  $\pi^*$  vacant orbitals. From Figure 1, we expect N1s (or O1s)  $\rightarrow \pi^*$  transition only for the OH-form (or NH-form). In the actual analysis, as described later, we must take account of the contribution from other resonance structures such as the zwitterionic structure shown in Scheme 1.

Such a study is also of interest as a chemical application of NEXAFS. So far no NEXAFS study of such tautomerism has been made, and it will be valuable to examine (i) how this phenomenon appears in NEXAFS, (ii) how detailed and reliable assignments can be made, and (iii) whether NEXAFS can be used for studying the tautomerism.

X-ray photoelectron spectroscopy (XPS) is another useful method for clarifying the chemical structure. Binding energies of the spectral features are sensitive to the chemical environment of the ionized atom, and it may be possible to distinguish the tautomers in SA derivatives. We note that the electronic transitions in these spectroscopies are fast ( $\sim 10^{-18}$  s)<sup>16</sup> compared to the hopping time of protons ( $\sim 10^{-10}$  s),<sup>17</sup> and the obtained results can be regarded as snapshots of the examined system.

In this work, we report a combined study of typical SA derivatives by NEXAFS and XPS spectroscopies. The assignments of the observed NEXAFS spectral features were performed by (i) the comparison with the spectra of related compounds, (ii) polarization dependence for oriented samples, and (iii) simulating the spectra by ab initio molecular orbital (MO) calculations of the core-excited states by the improved virtual orbital method<sup>18</sup> using the relaxed Hartree–Fock orbitals.<sup>19</sup> The method of calculation was successful in analyzing the NEXAFS spectra of polycyclic aromatic hydrocarbons,<sup>20</sup>

(13) Inabe, T.; Hoshino, N.; Mitani, T.; Maruyama, Y. *Bull. Chem. Soc. Jpn.* **1989**, *62*, 2245–2251.

(14) Stöhr, J. *NEXAFS Spectroscopy*; Springer-Verlag: Berlin, 1992; pp 162–210.

(15) Stöhr, J.; Outka, D. A. *Phys. Rev. B* **1987**, *36*, 7891–7905.

(16) Gadzuk, J. W. *Photoemission and the Electronic Properties of Surfaces*; Feuerbacher, B., Fitton, B., Wills, R. F., Eds.; Wiley Interscience: Chichester, 1978; pp 114–116.

(17) Takeda, S. Private communication.

(18) Hunt, W. J.; Goddard III, W. A. *Chem. Phys. Lett.* **1969**, *3*, 414–418.

(19) Kosugi, N. In *Atomic and Molecular Photoionization*; Yagishita, A., Sasaki, T., Eds.; Frontiers Science Series 18; Universal Academic Press: Tokyo, 1996; pp 89–98.

and it is interesting to apply it to the present more complex systems. The analyses of the NEXAFS spectra provided a rather clear picture about the tautomeric structures, demonstrating the usefulness of NEXAFS for investigating the tautomerism. The relative population of the OH- and NH-forms could be also deduced from the XPS spectra. Preliminary report about NEXAFS was published in ref 21.

## 2. Experimental Section

Five *N*-salicylideneaniline derivatives in Figure 2a–e were used. They are *N,N'*-disalicylidene-1,6-pyrenediamine (DSPY), *N,N'*-disalicylidene-*p*-phenylenediamine (BSP), *N*-(2-hydroxy-1-naphthylidene)-1-pyrenylamine (NPY), *N,N'*-di(2-hydroxy-1-naphthylidene)-*p*-phenylenediamine (DNP), and the complex between 7,7,8,8-tetracyanoquinodimethane (TCNQ) and DNP (DNP-TCNQ). All the materials were synthesized and purified as reported previously.<sup>8,9,12,13</sup> The compounds except for NPY have two H-bonded parts. By the combination of their protonic states, three tautomers can be considered, i.e., (A) [OH,OH]-, (B) [OH,NH]- or [NH,OH]-, and (C) [NH,NH]-forms shown in Figure 3 for DNP.

Previous studies by XD indicated that (i) DSPY exists only in the OH-form,<sup>10,13</sup> (ii) BSP, NPY, and DNP are in equilibrium between the OH and NH forms,<sup>8,9</sup> and (iii) DNP-TCNQ is mostly in the NH-form.<sup>12</sup> The results of XD also showed that the molecules studied here are planar except for DSPY where the three aromatic rings are twisted.<sup>13</sup> We also measured the NEXAFS and XPS spectra of two reference compounds, TCNQ and 2-(4'-methoxybenzylidene)aminofluorene (MBAF) in Figure 2. They were supplied from Tokyo Kasei Kogyo Co. Ltd.

The NEXAFS and XPS specimens were mostly prepared by vacuum evaporation at  $10^{-3}$  Pa on metal plates (Cu for DSPY, BSP, NPY, and DNP and Ni for TCNQ and MBAF). The film thickness was 100–150 nm as monitored by a quartz oscillator, and the evaporation rate was 0.2–0.5 nm/s. Since DNP-TCNQ decomposes on evaporation, its sample was prepared by scrubbing the sample powder on a scratched Ni plate.

Most NEXAFS experiments were carried out at the beamline 11A of Photon Factory at National Institute for High Energy Physics (KEK-PF). Synchrotron radiation from the storage ring was monochromatized by a Grasshopper monochromator with a grating of 2400 line/mm at a resolution of  $E/\Delta E \approx 1000$ . Monochromatized light was irradiated on the sample under vacuum of  $10^{-6}$  Pa, and the spectra were measured in the total electron yield mode. The photon flux was monitored as the hole drain current  $I_0$  from a Au-coated metal grid in the optical path. The emitted electrons from the sample were collected and amplified by a channeltron as the signal current  $I_s$ . These currents were converted to trains of pulses by a V-F converter, counted, and sent to a personal computer, and the NEXAFS spectrum was obtained as  $I_s/I_0$  vs photon energy. The spectra of MBAF were measured in a similar way at the beamline 2B1 of the UVSOR synchrotron radiation facility at Institute for Molecular Science using a Grasshopper monochromator with a grating of 2400 line/mm.

Most of the spectra were measured at an incidence angle of photons  $\theta \sim 55^\circ$  (so-called magic angle<sup>14,15</sup>), where  $\theta$  is measured from the substrate surface. At this value of  $\theta$ , possible effect of preferred molecular orientation can be removed. Auxiliary measurements at other  $\theta$  revealed that the spectra are mostly insensitive to  $\theta$ , suggesting random molecular orientation. As an exception, BSP showed weak  $\theta$  dependence, indicating preferred molecular orientation in the film. The energy calibration was carried out taking main peaks of TCNQ at the N *K*-edge and potassium sulfate ( $K_2SO_4$ ) at the O *K*-edge to be at 399.6 and 536.9 eV, respectively.<sup>22</sup>

The ab initio MO calculations with the minimal basis set were performed for (i) a planar SA molecule in the OH- and NH-forms, (ii) a nonplanar *N*-salicylidene-1-pyrenylamine (SPY) in the OH-form

(20) Oji, H.; Mitsumoto, R.; Ito, E.; Ishii, H.; Ouchi, Y.; Seki, K.; Kosugi, N. *J. Electron Spectrosc. Relat. Phenom.* **1996**, *78*, 383–386.

(21) Oichi, K.; Ito, E.; Seki, K.; Araki, T.; Narioka, S.; Ishii, H.; Okajima, T.; Yokoyama, T.; Ohta, T.; Inabe, T.; Maruyama, Y. *Jpn. J. Appl. Phys. Suppl.* **1993**, *32-2*, 818–820.

(22) Narioka, S.; Seki, K. Unpublished results.

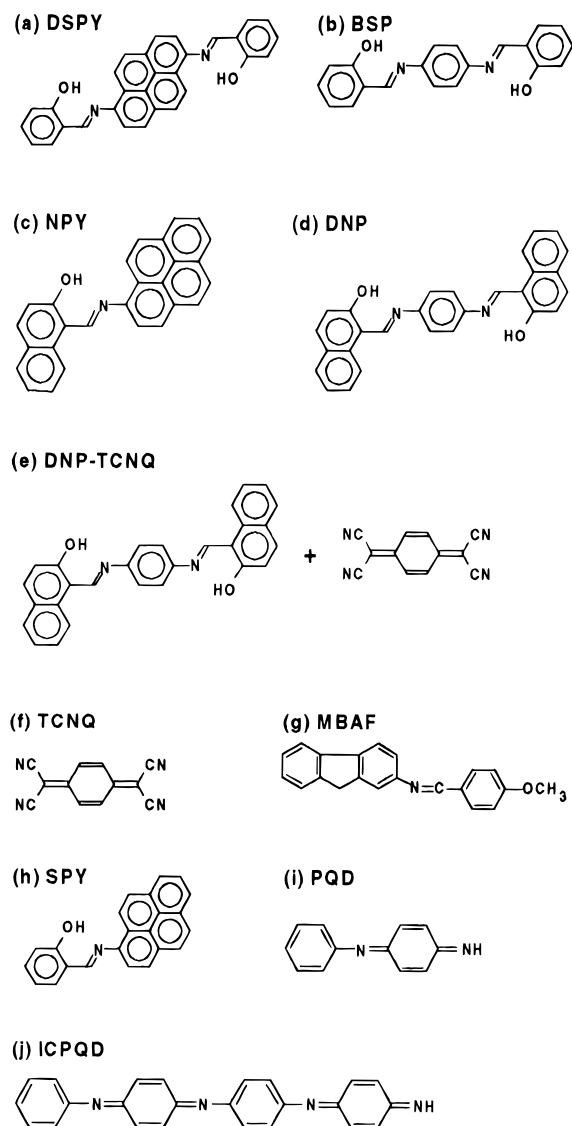


**Figure 2.** Molecular structures of the compounds studied: (a) DSPY, (b) BSP, (c) NPY, (d) DNP, (e) DNP-TCNQ, (f) TCNQ, and (g) MBAF, and the model compounds for calculations (h) SPY, (i) PQD, and (j) ICPQD.

(Figure 2h), and (iii) two reference compounds, *N*-phenyl-*p*-benzoquinone diimine (PQD) and *N*-{4-[(4-imino-2,5-cyclohexadienylidene)-amino]phenyl}-*N'*-phenyl-*p*-benzoquinone diimine (ICPQD) (Figure 2 (parts i and j)). We used the program GSCF3 coded by one of the authors (N.K.). The calculations of SA, PQD, and ICPQD were performed with the geometry optimized by a MOPAC semiempirical PM3<sup>23</sup> program. The geometry of SPY was taken from the XD study of DSPY.<sup>13</sup> For examining the possible effect of the ambiguity in geometry optimization, MO calculations for the OH-form of SA were also performed with the geometry optimized by ZINDO calculation and the geometry taken from the X-ray diffraction study of *N*-5-chlorosalicylideneaniline.<sup>3</sup> These geometries correspond to a variation of bond lengths and bond angles up to 0.03 Å and 2.5°, respectively. These variations little affected the obtained results.

Calculations for the core-ionized and core-excited states were carried out for the N and O atoms. The excitation energies for the core-excited states were obtained as the term value (ionization energy minus excitation energy) by applying the improved virtual orbital method<sup>18</sup> to the vacant orbital manifold of the core-ionized states. The transition intensities were obtained by calculating the transition dipole moments. From these results, the NEXAFS spectra were simulated as the weighted sum of Gaussian functions at excitation energies (FWHM = 0.9 eV and 1.5 eV for the N *K*- and O *K*-edges, respectively). The calculated

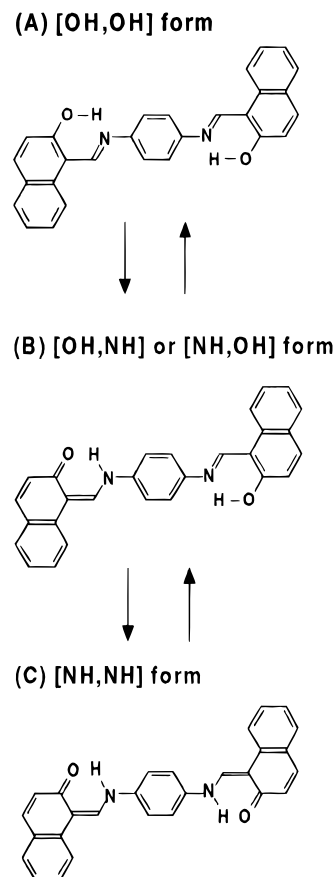


**Figure 3.** Three tautomeric forms in DNP.

$\sigma^*$  excitations appeared above the ionization energy, and they were not included in the simulation, since the present method neglects the mixing with the ionization continuum, and the obtained results will not be reliable.

XPS measurements were carried out on an Escalab 220i spectrometer (Vacuum Generators) below  $10^{-6}$  Pa using Mg *K* $\alpha$  X-ray source (15 kV, 20 mA). Peak positions and areas were determined by the curve fitting with the abscissa being determined by assuming the C1s main peak to be at 284.0 eV.

### 3. Results and Discussion

**1. NEXAFS Spectroscopy. (i) N *K*-Edge NEXAFS Spectra.** The N *K*-edge NEXAFS spectra of (a) DSPY, (b) BSP, (c) NPY, (d) DNP, (e) DNP-TCNQ, and (f) TCNQ are shown in Figure 4. The peak positions are listed in Table 1 with the assignments discussed later. The spectra of the SA derivatives show two sharp peaks 1 and 2, followed by weak features at higher energy. For NPY, the S/N ratio was not good, and the intensities of the peaks 1 and 2 were not well reproducible. Although the spectrum of DNP-TCNQ is fairly similar to that of TCNQ, indicating the large TCNQ contribution, the contribution from DNP can still be estimated as the difference (g) between these spectra (e) and (f).

The peaks 1, 2, and 4a in the spectra of BSP (b) are slightly stronger at grazing incidence than at normal incidence, indicating that they are  $\pi^*$  excitations. On the other hand, the peaks 4b, 5, and 6 showed opposite polarization dependence, indicating their  $\sigma^*$  character. This suggests that the features at  $\leq 403$  eV for other SA derivatives are also  $\pi^*$  excitations. This is confirmed by the spectra of oriented oxydianiline.<sup>24</sup> We here concentrate on the  $\pi^*$  excitations which are useful in discussing the tautomerism.

(23) Stewart, J. J. P. *J. Comput. Chem.* **1989**, *10*, 209–220.

(24) Murakami, T.; Ohta, T. Private communication.

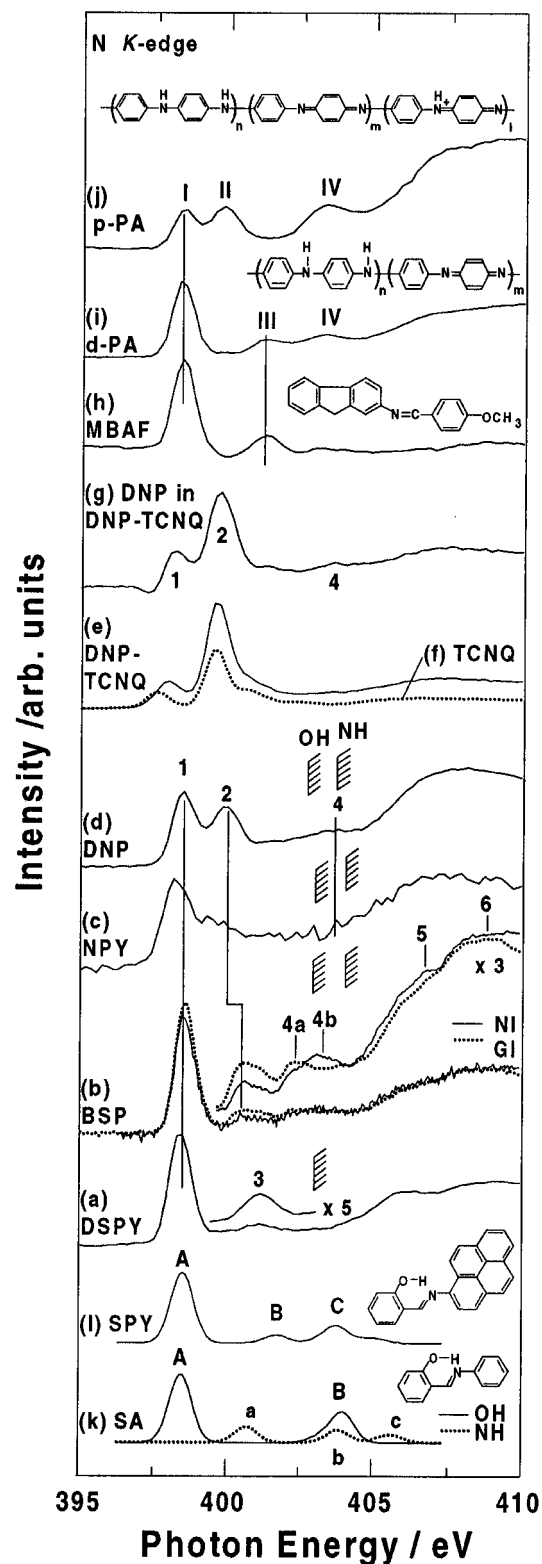


**Figure 4.** Upper part: N *K*-edge NEXAFS spectra of SA derivatives and related compounds: (a) DSPY, (b) BSP, (c) NPY, (d) DNP, (e) DNP-TCNQ, (f) TCNQ (dotted line), (g) difference spectrum between (e) and (f) showing the contribution from DNP in DNP-TCNQ, (h) MBAF and polyaniline (PA) in (i) the deprotonated form and (j) the N-protonated form (ref 25). For BSP, the spectra at the normal incidence (NI; solid line) and grazing incidence (GI; dotted line) are shown. Expanded spectra of DSPY and BSP are added above the spectra (a) and (b). The hatched lines denote the ionization potential obtained by the XPS spectra, assuming a work function of 4.5 eV (ref 29). Lower part: the simulated NEXAFS spectra by ab initio MO calculations for (k) SA in the OH-form (solid line) and the NH-form (dotted line), and (l) SPY in the OH-form.

For comparison, the spectra of MBAF (h) and two kinds of polyanilines (PA)<sup>25</sup> ((i) and (j)) are also shown in Figure 4. The peak I of PAs is aligned to the peak 1 of SA derivatives. For PA, the protonation to the N atoms can be changed by the treatment at various pH as shown in Table 2.<sup>25–27</sup> The spectrum (i) corresponds to the strongly deprotonated PA (d-PA), which is the mixture of the imine (=N–) and the amine (–NH–) forms. On the other hand, the spectrum (j) corresponds to the protonated PA (p-PA), which also contains the charged protonated (=N<sup>+</sup>H–) form converted from the imine form besides the imine and amine forms. The resultant structure of PAs are shown in Figure 4.

The structural correspondence between the PAs and SA derivatives can be assigned by Table 2. The OH-form of SA corresponds to the imine form of PA. The situation for the NH-form is more complex, since the NH-form tautomer is expressed by the resonance between the neutral and the zwitterionic structures. The neutral structure corresponds to the neutral structure of the amine form of PA, while the zwitterionic structure corresponds to both the zwitterionic structure and the charged protonated form of PA. We note that the contribution from the zwitterionic structure in PA will be small due to the lack of stabilization of the negative charge, in contrast to the case of SA where the negative charge is stabilized by the electronegative oxygen atom.

By protonation of PA, which converts the imine form to the charged protonated form,<sup>27</sup> the peaks I and III in the spectrum of d-PA become weak, and a new feature II appears between them. Thus, the former and the latter features were assigned to the transition at the imine N (=N–), and the charged protonated N (=N<sup>+</sup>H–) atoms, respectively.<sup>25</sup> The peaks I and II are also observed in the spectrum (h) of MBAF which has an imine nitrogen. Thus the peaks 1 and 3 of SA derivatives are ascribed to the OH-form and the peak 2 to the NH-form, respectively.

The intensities of peaks 1 and 2 give a measure of the relative population of the tautomers. DSPY shows only peaks 1 and 3, indicating that DSPY is in almost pure OH-form. The peak 2 ascribed to the NH-form becomes stronger in the order of BSP, NPY, DNP, and DNP-TCNQ. This ordering agrees with that suggested by XD.<sup>9–13</sup>

Detailed analysis by MO calculations for SA and SPY serves for checking the assignments described above. The simulated spectra (k) and (l) are shown in Figure 4, and Figure 5a depicts the  $\pi^*$  orbital patterns of the core-excited states of SA. The spectra (k) of the OH- and NH-forms of SA shown by the solid and dotted lines are aligned taking account of the difference of the N1s binding energies deduced by XPS (see section 3.2), and the peak A is aligned with the peak 1 of the observed spectra.

The peaks 1 and 2 correspond to the peaks A and a, which are the excitations to the LUMO of the OH- and NH-forms, respectively. This agrees with the assignments of these peaks to the OH- and NH-forms described above. The orbital pattern of A in Figure 5a shows large population at the imino group. The peak 1 can be assigned as the  $\pi^*(\text{N}=\text{C})$  excitation, in consistency with the assignment for the peak I of PA.<sup>25,28</sup>

The LUMO of the NH-form should contain the contribution from the zwitterionic structure in Table 2. The positive charge

(25) Szargan, R.; Hennig, C.; Hallmeier, K. H. *Synchrotron Radiat. News* **1996**, *9*, 34–35.

(26) Lintzelmann, A.; Scherrer, B.; Fink, J.; Meerholz, K.; Heine, J.; Sariciftci, N. S.; Kuzmany, H. *Syn. Metals* **1989**, *29*, E313–E319.

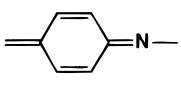
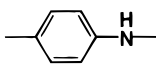
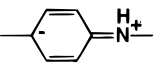
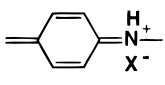
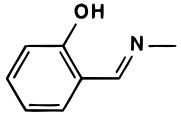
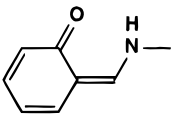
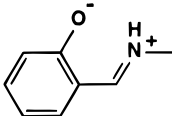
(27) Chiang, J. C.; MacDiarmid, A. G. *Syn. Metals* **1986**, *13*, 193–205.

(28) Hennig, C.; Hallmeier, K.-H.; Uhlrig, I.; Irl, S.; Schwarz, W. E.; Jung, C.; Hellwig, C.; Bach, A.; Möbius, M.; Beyer, L.; Szargan, R. *BESSY Annu. Rep.* **1993**, 172–174.

**Table 1.** Energies and Assignments of the Observed Peaks in the N *K*-Edge NEXAFS Spectra

	compd	DSPY	BSP	NPY	DNP	DNP in DNP-TCNQ	assignment
peak energy, eV	1	398.5	398.4	398.2	398.5	398.1	OH-form ( $\pi^*(\text{--N=C--})$ )
	2		400.5	399.5	400.0	399.7	NH-form ( $\pi^*(\text{--N}^+\text{=C--})$ )
	3	401					OH-form ( $\pi^*$ )
	4a		402		403.6	403.6	$\pi^* + \sigma^*$
	4b		403				
estimated structure		only OH	OH (+NH?)	OH + NH	OH + NH	NH + OH	

**Table 2.** Correspondence of the Forms between Polyaniline (PA) and Salicylideneaniline Derivatives (SAs)

	Peak	I, III	IV	II
PA		imine form	amine form	charged protonated form
Structure			neutral structure  ↔ zwitterionic structure 	
SAs		 OH-form	 neutral structure	 zwitterionic structure
Peak		1, 3	2	

on the N atom leads to high N1s  $\rightarrow \pi^*$  transition energy. The orbital pattern of a is fairly similar to that of A, corresponding to the similar bonding patterns in the OH-form and the zwitterionic structure.

As described above, the peak 3 in the spectrum of DSPY can be attributed to the OH-form. It corresponds to the peak B in the simulated spectrum of SPY, which is at lower energy than the corresponding peak B in the simulated spectrum of SA. This shift can be ascribed to the low energy of the  $\pi^*$  orbital in DSPY and SPY due to the delocalization in the large central pyrenyl ring. MBAF also has a ring of comparable size with DSPY and SPY. This explains the similar energies of peaks III of MBAF and peak 3 of DSPY. On the other hand, the peak III in d-PA, which was ascribed to a delocalized  $\pi^*(\text{=N}\cdot\cdot)$  orbital,<sup>25</sup> appears at similar energy to those of DSPY and MBAF, although d-PA has small phenyl rings. The MO calculations for the two model compounds of the imine form of PA (PQD and ICPQD in Figure 2 (parts i and j)) indicated that the excitations corresponding to B in PQD and ICPQD are at almost the same energy as that of SA and SPY, respectively. Thus the low energy of the peak III in d-PA can be ascribed to the delocalization along the chain.

The analysis of the peaks of SA derivatives and PAs at higher energies is not simple. Firstly, the simulated spectra of SA (Figure 4k) indicate that both OH- and NH-forms have the  $\pi^*$  excitations (B and b) in this energy region. Further, the spectrum of BSP shows that both  $\pi^*$  (peak 4a) and  $\sigma^*$  (peak 4b) excitations exist in this region. Secondly, the ionization

potentials are also in this energy range. The deduced values from XPS spectra are indicated by the hatched lines in Figure 4 for the OH- and NH-forms, respectively, assuming a representative value of the work function of 4.5 eV for organic solids.<sup>29</sup> We see that even the peaks 4 and IV may be above the ionization energy, and it becomes dangerous to discuss these excitations using the present calculations, which neglects the mixing with the continuum states.

Finally, we examine the possible interaction of the two tautomeric parts in DSPY, BSP, DNP, and DNP-TCNQ. The similarity of their spectra with those of NPY and MBAF with a single tautomeric part indicates only weak interaction. This was also confirmed by CNDO/S MO calculations of BSP, NPY, and DNP using equivalent core approximation<sup>30–32</sup> at the N *K*- and O *K*-edges.

**(ii) O *K*-Edge NEXAFS Spectra.** The O *K*-edge NEXAFS spectra of the five SA derivatives (a)–(e) are shown in Figure 6. As in the case of the N *K*-edge, the relative spectral intensity for NPY was not well reproducible. The previous studies<sup>33,34</sup>

(29) Kotani, M.; Akamatu, H. *Discussion Faraday Soc.* **1970**, *51*, 94–101.

(30) Davis, D. W.; Shirley, D. A. *Chem. Phys. Lett.* **1972**, *15*, 185–190.

(31) Seki, K.; Morisada, I.; Edamatsu, K.; Tanaka, H.; Yanagi, H.; Yokoyama, T.; Ohta, T. *Phys. Scr.* **1990**, *41*, 172–176.

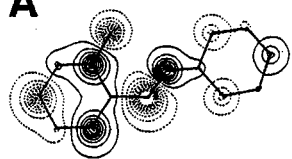
(32) Yokoyama, T.; Seki, K.; Morisada, I.; Edamatsu, K.; Ohta, T. *Phys. Scr.* **1990**, *41*, 189–192.

(33) Ishii, I.; Hitchcock, A. P. *J. Electron Spectrosc. Relat. Phenom.* **1988**, *46*, 55–84.

## (a) N K-edge

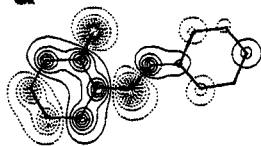
## OH-form

A

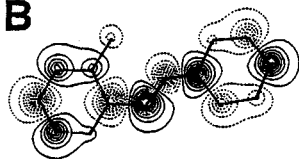


## NH-form

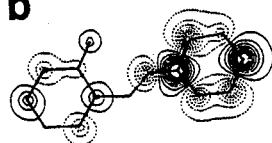
a



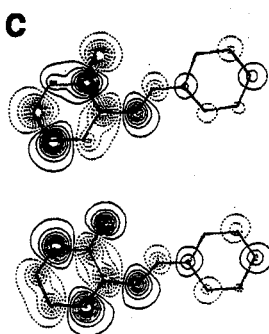
B



b



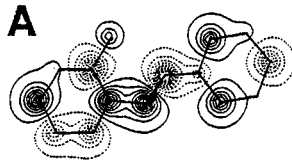
c



## (b) O K-edge

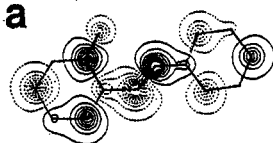
## OH-form

A

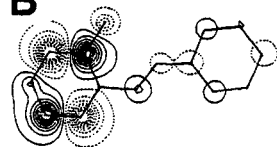


## NH-form

a



B



b

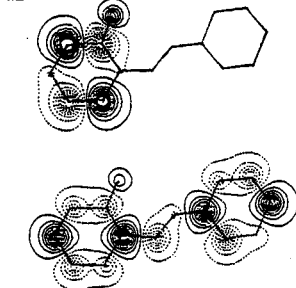


**Figure 5.**  $\pi^*$  orbital patterns of (a) the N1s- and (b) the O1s-excited states of SA corresponding to the features in the simulated spectra in Figures 4 and 6.

indicate that (1) the peak at about 539eV is due to the  $\sigma^*(\text{O}-\text{C})$  excitation and (2)  $\sigma^*(\text{O}-\text{H})$  and  $\pi^*$  excitations are expected at lower energy. The positions and the assignments of the  $\pi^*$

(34) Francis, J. T.; Hitchcock, A. P. *J. Phys. Chem.* **1992**, 95, 6598–6610.

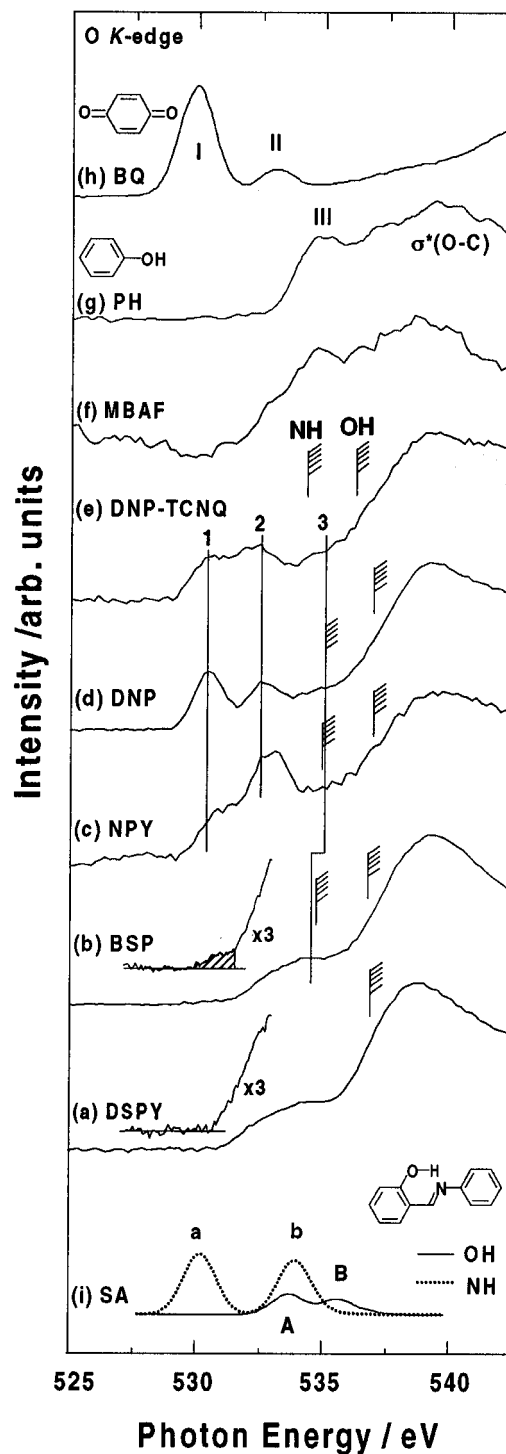


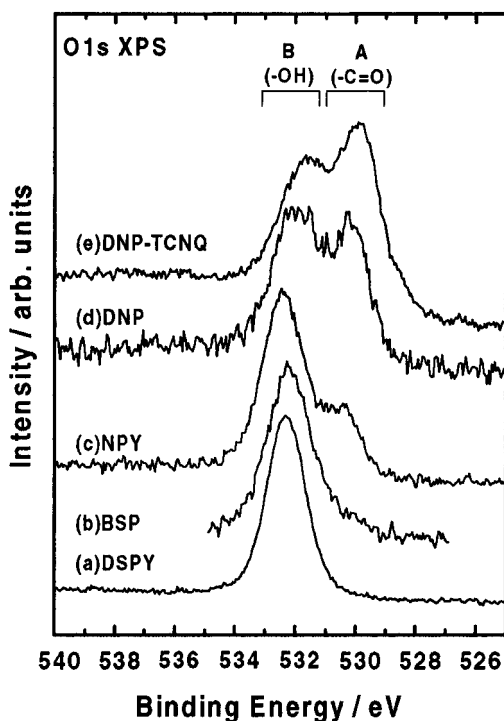
**Figure 6.** Upper part: O K-edge NEXAFS spectra of (a) DSPY, (b) BSP, (c) NPY, (d) DNP, and (e) DNP-TCNQ, (f) MBAF, and the electron energy loss spectra of gas phase phenol (PH) (g), and *p*-benzoquinone (BQ) (h) (ref 34). The hatched lines denote the ionization potential obtained by the XPS spectra, assuming a work function of 4.5 eV (ref 29). Lower part: (i) the simulated spectra by ab initio MO calculations of SA in the OH-form (solid line) and the NH-form (dotted line).

peaks are listed in Table 3. For comparison, the spectrum of MBAF (f), the reported gas phase electron energy loss spectra of phenol (PH) (g) and *p*-benzoquinone (BQ) (h),<sup>34</sup> and the simulated spectra of SA (i) are also shown.

BQ has two C=O groups, and the peaks I and II were assigned to the transitions from the O1s level to the  $\pi^*$  orbitals

**Table 3.** Energies and Assignments of the Observed Peaks in the O *K*-Edge NEXAFS Spectra

	compd	DSPY	BSP	NPY	DNP	DNP-TCNQ	assignment
peak energy, eV	1		530.8	530.7	530.2	530.3	NH-form ( $\pi^*(C=O)$ )
	2			532.8	532.5	532.3	NH-form
	3	534.5	534.5		535.5	535	OH-form
estimated structure		only OH	OH (+NH)	OH + NH	OH + NH	NH + OH	

**Figure 7.** O1s XPS spectra of (a) DSPY, (b) BSP, (c) NPY, (d) DNP, and (e) DNP-TCNQ.

derived from the O2p<sub>z</sub> orbital and the  $\pi^*$  orbitals of benzene.<sup>34</sup> On the other hand, PH has a OH group, and the feature III was attributed to the  $\sigma^*(OH)$  excitation with possible contribution from 1s  $\rightarrow \pi^*$  excitation.<sup>34</sup> The spectrum of MBAF resembles to that of PH expect for the tail to lower energy.

The features 1 and 2 in the spectra of NPY, DNP, and DNP-TCNQ correspond to the peaks I and II of BQ, respectively, and can be ascribed to the NH-form with C=O double bond-(s). The broad shoulder 3 of SA derivatives corresponds to the feature III of PH and is attributed to the  $\sigma^*(O-H) + \pi^*$  excitations in the OH-form.

The amount of the NH-form can be estimated from the intensity of the peak 1. DSPY does not show this peak, showing the absence of the NH-form. The spectrum of BSP shows a small rise at about 531 eV in the expanded spectrum (hatched region), suggesting that BSP has a small but finite amount of the NH-form. The other data indicates the increase of the NH-form in the order of NPY, DNP, and DNP-TCNQ. This trend agrees with that from the N *K*-edge NEXAFS and XD.<sup>9-13</sup>

More detailed analysis of the spectra can be performed by using the simulated spectra (i) of the OH- and NH-forms of SA. They are aligned using the difference of O1s binding energies deduced by XPS (section 3.2). The result for the OH-form of SPY was similar to that of SA. The calculated orbital patterns of the core excited-states are shown in Figure 5b. The ionization potentials in both tautomers (hatched lines in Figure 6) are slightly higher than the energy of the second  $\pi^*$  transition in each tautomer, ensuring that we can use these simulated spectra for the assignments.

The peaks 1 and 2 should correspond to the peaks a and b in the simulated spectrum of the NH-form, respectively. The

**Table 4.** Binding Energies and Intensity Ratios of the Observed Peaks in the O1s XPS Spectra by the Curve Fitting

assignment	binding energy, eV		ratio
	A NH form	B OH form	NH form:OH form
DSPY		532.3	0:100
BSP	530.2	532.2	7:93
NPY	530.4	532.4	25:75
DNP	530.5	532.4	40:60
DNP-TCNQ	529.8	531.7	60:40

**Table 5.** Binding Energies and Intensity Ratios of the Observed Peaks in the N1s XPS Spectra by the Curve Fitting

assignment	binding energy, eV		ratio
	A OH form	B NH form	OH form:NH form
DSPY	398.5		100:0
BSP	398.4	399.5	96:4
NPY	398.5	399.5	80:20
DNP	398.2	399.2	50:50

orbital patterns in Figure 5b indicate that the final states are formed by the mixing of the O2p<sub>z</sub> orbital and the benzene  $\pi^*$  orbital. Such delocalized MO patterns were also reported for BQ.<sup>34</sup>

The peak 3 in the spectra of BSP showed little polarization dependence. This suggests the mixed contribution from the  $\pi^*$  and  $\sigma^*$  excitations, although the calculation did not show the  $\sigma^*$  transitions in this energy region. This agrees with the reported  $\sigma^*(O-H)$  and  $\pi^*$  nature of the peak II of PH.<sup>34</sup> The  $\pi^*$  component should correspond to the peaks A and B in the simulated spectrum and overlap with the  $\sigma^*(O-H)$  excitation forms a broad peak. The orbital patterns in Figure 5b indicate that the final state for A is well delocalized, while that for B is mostly in the 2-hydroxyphenyl ring. The excitation A corresponds to the resonance structure with the positively charged oxygen  $H-O^+=C$ . This explains the similarity of the orbital patterns of a and A.

Thus the assignments by MO calculations are consistent with those from the spectra of related compounds. The good correspondence with the observed results at both the N *K*- and O *K*-edges demonstrates the usefulness of the present theoretical analysis for assigning the spectral features for the complex systems.

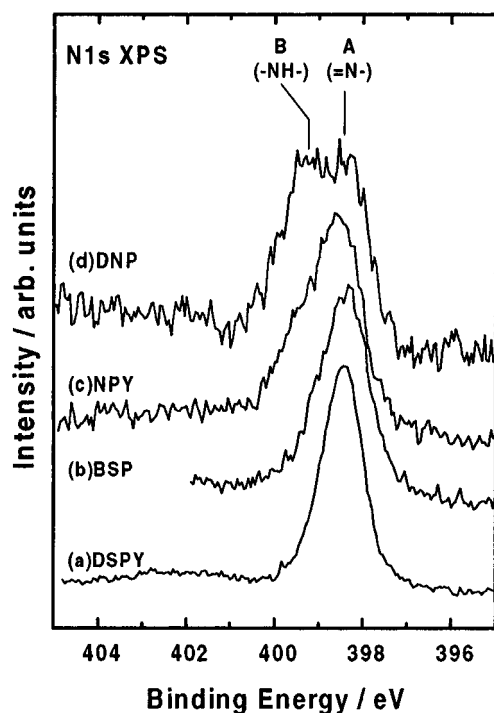
**2. XPS Spectroscopy.** The XPS results offer an independent way of examining the tautomerism. In Figure 7, the O1s XPS spectra of SA derivatives are shown. The spectra of BSP, NPY, DNP, and DNP-TCNQ can be decomposed into two peaks A and B. On the other hand, the spectrum of DSPY shows only peak B. Comparison with the results for BQ (530.8 eV) and *p*-hydroquinone (HO-C<sub>6</sub>H<sub>4</sub>-OH) (532.2 eV)<sup>35</sup> ascribes the peak A to the C=O group in the NH-form and the peak B to the OH group in the OH-form, respectively.

In Figure 8, the N1s XPS spectra of four SA derivatives are shown. The spectrum of DNP-TCNQ is not shown, due to the difficulty in subtracting the contribution from TCNQ. We can again reproduce these spectra as the combination of peaks A and B, which can be assigned to the N atoms in the OH-form

(35) Ohta, T.; Yamada, M.; Kuroda, H. *Bull. Chem. Soc. Jpn.* **1974**, *47*, 1158-1161.

**Table 6.** Comparison of the Results for the Hydrogen-Bonded Structures of SA Derivatives by Various Methods

compound	NEXAFS		XPS		X-ray diffraction <sup>a</sup>	
	N K-edge	O K-edge	N1s	O1s	D-synthesis	$r(\text{C}-\text{O})$ , pm
DSPY	only OH-form		only OH-form		H near O	135.6
BSP	OH-form (major) +NH-form (minor)		OH-form	OH-form	H near O	134.9
NPY	OH-form + NH-form		96% OH-form	93% OH-form	(+ H near N) broad distribution between O and N	131.9
DNP	OH-form + NH-form comparable amount		80% OH-form	75% OH-form	H near O + H near N	132.2
DNP-TCNQ	NH-form + OH-form	difficult to estimate	50% difficult to estimate	60% OH-form	H near N	129.0
TCNQ				40%		

<sup>a</sup> References 9 and 12.**Figure 8.** N1s XPS spectra of (a) DSPY, (b) BSP, (c) NPY, and (d) DNP.

(=N-) and the NH-form (-NH-), respectively, by the comparison with the spectrum of metal-free tetraphenylporphyrin.<sup>36</sup>

The relative amounts of tautomers can be estimated from these spectra by the curve fitting. They are summarized in Tables 4 and 5. The results from N1s and O1s spectra are similar and also consistent with those from NEXAFS. In particular, the small yet finite population of the NH-form in BSP agrees with the results of NEXAFS. These results show that quantitative estimation could be successfully performed by XPS.

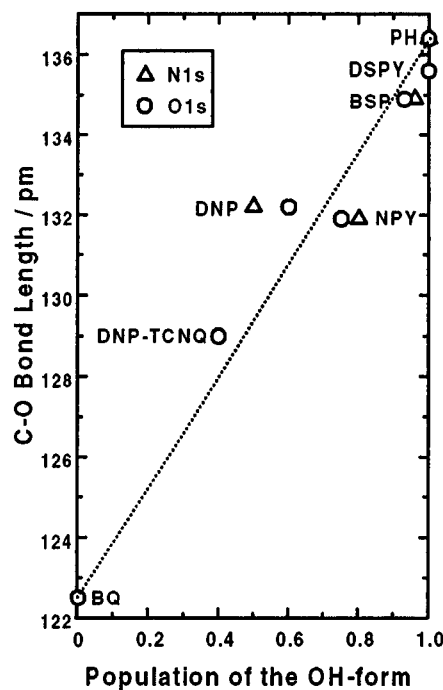
**3. Comparison of the H-Bonded Structure Estimated by Various Methods.** Now we compare the results by various methods summarized in Table 6. The left column of XD shows the results from D-synthesis, which was already discussed in the preceding sections. The right column lists the bond lengths of the C-O bond,  $r(\text{C}-\text{O})$ . In general,  $r(\text{C}-\text{O})$  is long for a single bond (e.g., 136.4 pm in PH<sup>37</sup>), while it is short for a double bond (e.g., 122.5 pm<sup>38</sup> in BQ).

The  $r(\text{C}-\text{O})$  value by XD is the time average in the mixed OH- and NH-forms. It should be long for a pure OH-form and

(36) Niwa, Y.; Kobayashi, H.; Tsuchiya, T. *J. Chem. Phys.* **1974**, *60*, 799–807.

(37) Pedersen, T.; Larsen, N. W.; Nygaard, L. *J. Mol. Struct.* **1969**, *4*, 59–77.

(38) Hagen, K.; Hedberg, K. *J. Chem. Phys.* **1973**, *59*, 158–162.

**Figure 9.** Correlation between the population of the OH-form estimated by XPS and the C-O bond length determined by X-ray diffraction (ref 9 and 12).

will become shorter with increasing weight of the NH-form. The value of DSPY (135.6 pm<sup>13</sup>) is similar to that of PH, indicating that DSPY is almost purely in the OH-form. On the other hand, DNP-TCNQ has the shortest  $r(\text{C}-\text{O})$  among the compounds studied, indicating the largest contribution from the NH-form. NPY and DNP have similar  $r(\text{C}-\text{O})$  (131.9 pm and 132.2 pm, respectively<sup>9</sup>), which are intermediate between those of DSPY and DNP-TCNQ. From these data, we can deduce increasing population of the NH-form in the order of DSPY < BSP < NPY  $\approx$  DNP < DNP-TCNQ.

In Table 6, the results from NEXAFS, XPS, and XD correspond well except for the following two points. Firstly, XPS shows different populations in NPY and DNP, while XD indicates similar structure. The origin of this discrepancy is not clear at present. Secondly, the O1s XPS indicates considerable population of the OH-form in DNP-TCNQ, while D-synthesis suggests almost pure NH-form. For examining this discrepancy, the correlation between  $r(\text{C}-\text{O})$  and the OH-form population by XPS is shown in Figure 9. It indicates a rather good linear relation. In particular,  $r(\text{C}-\text{O})$  in DNP-TCNQ is significantly longer than that of a pure double bond in BQ, suggesting at least some contribution from the OH-form. Thus the NEXAFS and XPS data firmly established the tautomeric structures of these SA derivatives and even corrected the XD result suffering from the limited sensitivity to the H atom.



Additional information is also available from the reported proton NMR studies.<sup>39</sup> In BSP, the relaxation time of NMR gave the energy differences of 4.0 kJ/mol between the (A) and (B) forms in Figure 3 and 8.5 kJ/mol between the (B) and (C) forms.<sup>39</sup> If we assume Boltzmann distribution, the population of the OH-form is 85%. For DNP, the corresponding energy differences of 0.38 and 0.9 kJ/mol result in the OH-form population of 56%.<sup>39</sup> These values agree well with the results from XPS.

#### 4. Conclusion

In this work, we studied five *N*-salicylideneaniline (SA) derivatives by NEXAFS and XPS spectroscopies. The observed structures in the NEXAFS spectra could be assigned in detail, by the comparison with reference compounds and the simulation by ab initio calculations, demonstrating the usefulness of this type of MO calculations for analyzing the NEXAFS spectra of such complex molecules. By examining the peak intensities, the tautomeric structures of SA derivatives could be deduced.

The observed N1s and O1s XPS spectra showed double-peaked features characteristic of the mixture of the OH- and NH-forms. By the curve fitting of these spectra, the ratio between the OH- and NH-forms could be determined quantitatively.

These results by NEXAFS and XPS spectroscopies are generally consistent with those estimated from XD. DSPY contains only the OH-form, and the remaining four compounds

contain both tautomers, with the relative population of the NH-form increasing in the order of BSP, NPY, DNP, and DNP-TCNQ. As an exceptional discrepancy from the estimation by XD, XPS indicated comparable population of the OH- and NH-forms in DNP-TCNQ. This conclusion was confirmed by the good correlation with the C–O bond length.

The two spectroscopies thus offered independent confirmation for the somewhat ambiguous results previously obtained and even more reliable and detailed information about the tautomerism in these compounds. The present work has also demonstrated the usefulness of NEXAFS for studying tautomerism. We expect that this method and XPS are particularly useful for amorphous states and ultrathin films, to which other methods such as XD and IR spectroscopy are difficult to apply.

**Acknowledgment.** We are grateful to Prof. Sadamu Takeda of Gunma University for helpful discussion and to Mr. Takashi Murakami for the communication of the data of oxidianiline. E.I. thanks Research Fellowship of the Japan Society for Promotion of Science for Young Scientists. This work was supported in part by the Grant-in-Aid from the Ministry of Science, Education, Sports, and Culture of Japan (Nos. 04403001, 07NP0303, and 07CE2004) and the Venture Business Laboratory Project "Advanced Nanoprocess Technologies" at Nagoya University. This work was performed under the approval of the Photon Factory Program Advisory Committee (Nos. 90–127, 91–198, and 93G324) and Joint Studies Program of UVSOR Facility at Institute for Molecular Science (No. 8–518).

JA9641362

(39) Takeda, S.; Chihara, H.; Inabe, T.; Mitani, T.; Maruyama, Y. *Chem. Phys. Lett.* **1992**, *189*, 13–17.